Hindawi
Advances in Materials Science and Engineering
Volume 2019, Article ID 3764395, 10 pages
https://doi.org/10.1155/2019/3764395

Research Article

Strain Effects on the Band Gap and Diameter of CdSe Core and CdSe/ZnS Core/Shell Quantum Dots at Any Temperature

Md. Rezaul Karim,[1,2] Mesut Balaban,[3] and Hilmi Ünlü[1]

[1]*İstanbul Technical University, Faculty of Science and Letters, Department of Physics Engineering, 34485 Maslak, İstanbul, Turkey*
[2]*Department of Physics, Dhaka University of Engineering & Technology, Gazipur-1700, Bangladesh*
[3]*Yıldız Technical University, Faculty of Science, Department of Physics, 34220 Esenler, İstanbul, Turkey*

Correspondence should be addressed to Hilmi Ünlü; hunlu@itu.edu.tr

Received 3 May 2019; Revised 29 July 2019; Accepted 9 August 2019; Published 22 September 2019

Academic Editor: Luca De Stefano

We present the results of an experimental study about strain effects on the core band gap and diameter of spherical bare CdSe core and CdSe/ZnS core/shell quantum dots (QDs) synthesized by using a colloidal technique at varying temperatures. Structural characterizations were made by using X-ray diffraction (XRD) and high-resolution transmission electron microscopy (HRTEM) techniques. Optical characterizations were made by using UV-Vis absorption and fluorescence emission spectroscopies. The XRD analysis suggests that the synthesized bare CdSe core and CdSe/ZnS core/shell QDs have zinc blende crystal structure. HRTEM results indicate that the CdSe core and CdSe/ZnS QDs have average particle sizes about 3.50 nm and 4.84 nm, respectively. Furthermore, compressive strain causes an increase (decrease) in the core band gap (diameter) of spherical CdSe/ZnS core/shell QDs at any temperature. An elastic strain-modified effective mass approximation (EMA) predicts that there is a parabolic decrease (increase) in the core band gap (diameter) of QDs with temperature. The diameter of spherical bare CdSe core and CdSe/ZnS core/shell QDs calculated by using the strain-modified EMA, with core band gap extracted from absorption spectra, are in excellent agreement with the HRTEM data.

1. Introduction

Group II-VI compound semiconductor-based spherical bare CdSe core and CdSe/ZnS core/shell quantum dots (QDs) have generated much interest among device scientists and engineers because of their potential use in fabrication of new generation solar cells, light-emitting diodes (LEDs), fluorescent biosensors etc. [1–6]. When CdSe and ZnS are brought in contact to form a heterostructure CdSe/ZnS core/shell QD by using a crystal growth technique, conduction and valence band edges of core and shell regions are aligned in a way that an electron-hole pair excited near the heterointerface (Type I structure) tend to localize in the core region. The exciton energy in Type I core/shell QDs is the result of a direct exciton transition inside the core. Figure 1 shows the schematic cross-sectional view, formation, and band diagram of a spherical heterostructure. The difference in the band gaps of CdSe and ZnS is accommodated by the spike ΔE_c in conduction band and the potential step ΔE_v in valence band at the heterointerface, causing the electron and hole confinement in the CdSe core, creating an electron-hole pair there.

As a nanoscale heterostructure core/shell QD is formed between two semiconductors with different lattice constants and thermal expansion coefficients, an elastic strain develops across the heterointerface. The elastic strain can modify the structural, electronic, optical and dielectric properties of constituent semiconductors in a way that is not seen in two-dimensional quantum wells and superlattices. If the core lattice constant is greater than the shell lattice constant, the core (shell) region will be under compressive (tensile) elastic strain, resulting in an increase (decrease) in the core (shell) band gap energy and a decrease (increase) in the diameter. Reliable and precise determination of the magnitude of

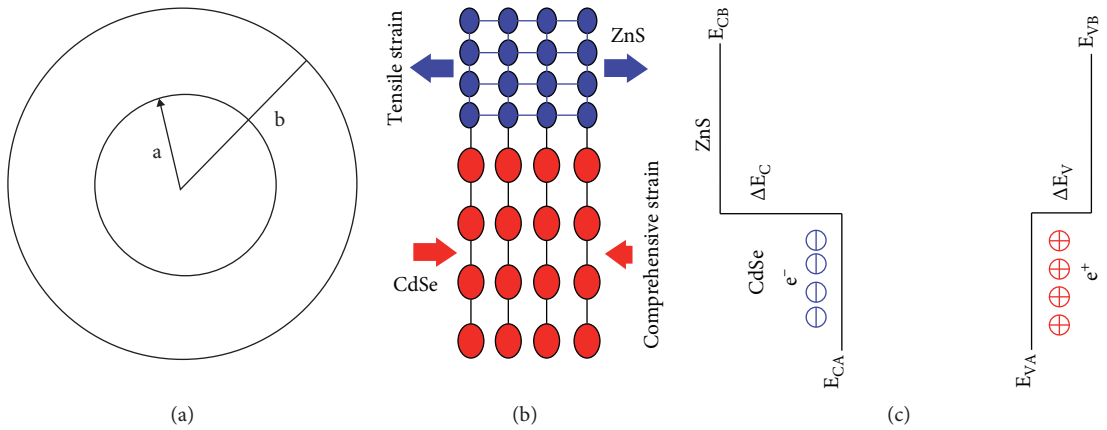

Figure 1: Schematic cross-sectional view of core/shell (a), interface strain (b), and band diagram (c) of pseudomorphic CdSe/ZnS heterostructure core/shell quantum dot.

interface strain effects on structural and electronic properties of core/shell QDs become important in determining their tunable properties such as the core band gap and diameter, which are essential for predicting their potential as electronic and optical devices.

The aim of this work is to prove that elastic strain has parabolic effects on the band gap and diameter of bare CdSe core and CdSe/ZnS core/shell QDs as a function of temperature, which were synthesized by using a colloidal technique and characterized by using X-ray diffraction (XRD), high-resolution transmission electron microscopy (HRTEM), UV-Vis absorption, and fluorescence emission techniques, respectively. Colloidal synthesis of CdSe core and CdSe/ZnS core/shell QDs is summarized in Section 2. The results of HRTEM and XRD characterizations of the size of QDs will be discussed in Sections 3.1 and 3.2, respectively. The optical UV-Vis absorption and fluorescence emission spectral analysis of QDs will be presented in Sections 3.3 and 3.4, respectively. The core diameter of QDs calculated by using strain–modified two-band effective mass approximation, with the core band gap extracted from UV-Vis absorption spectra, will be compared with the results of HRTEM analysis.

2. Synthesis of CdSe Core and CdSe/ZnS Core/Shell QDs

The bare CdSe core quantum dots were synthesized by using modifications of the method of He and Gu [7]. During the synthesis reaction, 0.69 g cadmium acetate and 2.5 mL oleic acid were dissolved with 10 mL phenyl ether in a three-neck flask. The reaction mixture was heated to 140°C under stirring and continuous nitrogen flow and then the mixture was cooled to room temperature. Then 3 mL 1M TOPSe was added to the mixture rapidly and heated to high temperatures (e.g., 160°C and 170°C) for 1 to 20 minutes of reaction times.

The CdSe/ZnS core/shell QDs were synthesized by using modification of the technique by Zhu et al. [8]. In brief, the resulting core solution (reaction for 1 to 20 minutes), $Zn(OAc)_2$-$2H_2O$ (0.085 mmol), and S powder (0.085 mmol) were mixed together in a reaction vessel. The reaction volume was adjusted to 15 mL by adding paraffin liquid. Next, with stirring, the mixture was degassed at 80°C for about 20 minutes. Afterwards, temperature was set to 160°C to 170°C for the capping of CdSe core with ZnS under N_2 atmosphere. The reaction mixture was cooled down to 300 K after 50 minutes and then 1 mL aliquot crude solution was washed with methanol and isolated by centrifugation to remove excess insoluble organics and salts that may have formed during the reaction. After the fine isolation of growth CdSe/ZnS core/shell QDs, the precipitation was dissolved with different volume of hexane. The reaction was monitored with Shimadzu UV-Vis NIR absorption spectrometer with aliquots taken at different time and temperature.

3. Results and Discussion

3.1. HRTEM Characterization Results. The synthesized bare CdSe core and CdSe/ZnS core/shell nanocrystals were characterized by using high-resolution transmission electron macroscopy (HRTEM) with JEOL JEM-ARM200CFEG UHR-TEM at an acceleration voltage of 200 kV. A drop of dispersed nanocrystals diluted in n-hexane dropped over an amorphous carbon substrate supported on a copper grid of 400 mesh for taking images. Figures 2(a) and 2(b) show the HRTEM images of bare CdSe core NCs synthesized at 160°C for 1 and 20 minutes of reaction time, respectively. Figures 2(c) and 2(d) show the HRTEM images of CdSe/ZnS core/shell NCs synthesized at 160°C and 170°C for 20 minutes of reaction time, respectively. HRTEM images shown in Figure 2 indicate that both the bare CdSe core and CdSe/ZnS core/Shell NCs are uniform in size and shape. The nanocrystal size becomes larger as reaction time is increased. We estimate the average diameters of bare CdSe core and CdSe/ZnS core/shell NCs are 3.50 nm and 4.84 nm, respectively.

One can estimate the thickness of ZnS shell by subtracting the size of the bare CdSe core from that of the CdSe/ZnS core/shell QD. However, since changes in the core size during the shell deposition is inevitable due to strain across the core/shell interface, TEM images after the shell

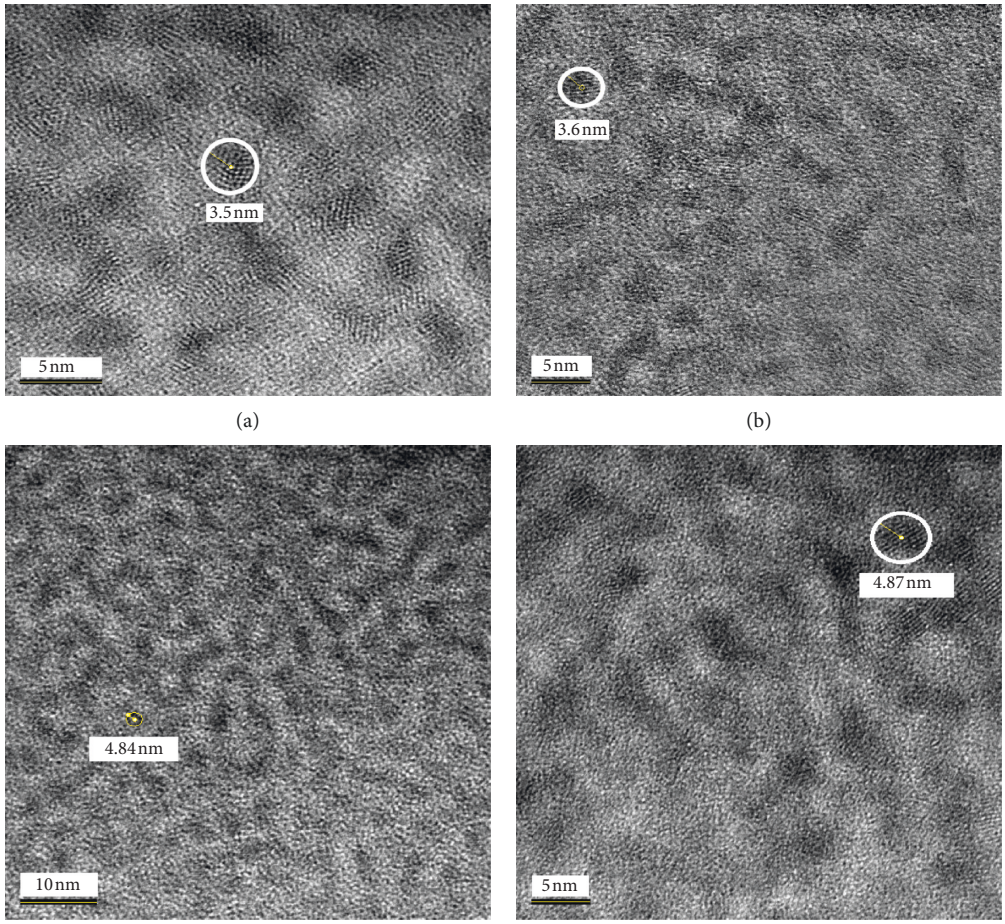

Figure 2: HRTEM images of bare CdSe core QD synthesized at 160°C for 1 min (a) and 20 min (b) reaction times, and of CdSe/ZnS core/shell QD synthesized at 160°C (c) and 170°C (d) for 20 min reaction time, respectively.

deposition may not be a reliable reference to estimate the exact core size.

3.2. XRD Characterization Results. X-rays diffraction technique is used for determining the mean size of single crystal nanoparticles and nanocrystallites in bulk materials. X'Pert³ MRD (XL) X-ray diffractometer operating at 45 kV/40 mA using copper Kα line ($\lambda = 0.15406$ nm) was used in the structural characterization of the bare CdSe core and CdSe/ZnS core/shell nanocrystals. Figure 3 shows the comparison of the XRD patterns of bare CdSe core and core/shell CdSe/ZnS NCs both prepared at 170°C. The XRD spectra for samples were fitted by a Gaussian profile for each peak and a quadratic function for the background.

The XRD pattern of bare CdSe core NCs exhibits broad peaks at 2θ values of 25° related to (111), 42° to (220), and 48° to (311) crystalline plane for low-temperature-synthesized zinc-blende CdSe JCPDS data base (Joint Committee on Powder Diffraction Standards file No. 77-2100). There is a slight shift in the XRD pattern after capping the CdSe core with ZnS shell to form a CdSe/ZnS core/shell NC. The broad nature of the peaks suggests nanocrystalline particles. Here, we point out that there is no drastic change in the diffraction

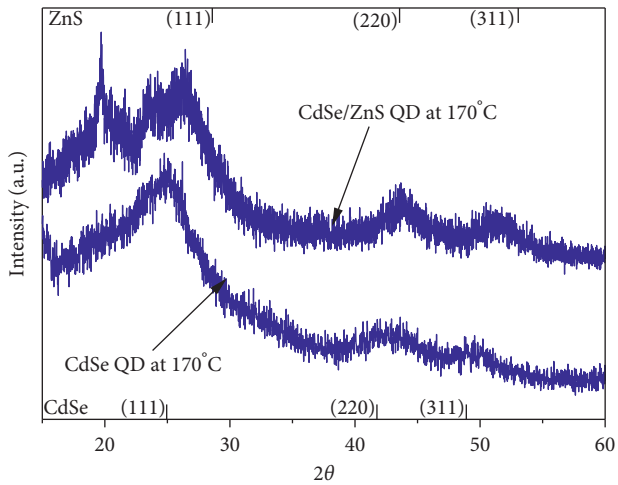

Figure 3: The XRD patterns of (a) bare CdSe core QD prepared at 170°C for 2 min and at 190°C for 15 min, respectively, and (b) core/shell CdSe/ZnS QDs and corresponding bare CdSe core QDs prepared at 170°C for 2 min reaction time.

patterns of CdSe/ZnS core/shell NCs relative to that of bare CdSe core NCs. This is due to the fact that the thickness of ZnS shell layer is very small (about one monolayer).

Although during purification almost all of paraffin was extracted from aliquots, paraffin as an amorphous element suppresses peaks in the XRD pattern. The XRD patterns in Figure 3 provide strong evidence that bare CdSe core and core/shell CdSe/ZnS NCs have a zinc-blende (ZB) crystal structure. No reflection pattern from wurtzite lattice structure (102) at $2\theta \approx 35^{\circ}$ and (103) at $2\theta \approx 46^{\circ}$ is found in the XRD pattern, which is considered as further evidence that bare CdSe core and CdSe/ZnS core/shell NCs have a ZB crystal structure.

3.3. UV-Vis Absorption and PL Emission Characterization Results. Figures 4(a) and 4(b) compare the growth temperature effects on the absorption and emission spectra of bare CdSe core QDs synthesized at 155°C, 165°C, and 175°C for 5 and 10 minutes of reaction times.

The position of the maximum wavelength at which absorption and emission coefficients of bare CdSe core NCs are maximum tends to slightly shift to higher wavelengths as temperature is increased. Emission peaks vary between 507 nm to 542 nm for different reaction times.

Figures 5(a) and 5(b) compare the effect of growth temperature on the absorption and emission coefficients of CdSe/ZnS core/shell QDs synthesized at 160°C, and 170°C for 1, 5 10, and 20 minutes of reaction times. The emission peaks of core/shell NCs range from 550 to 570 nm, corresponding to the full-width at half maximum (FWHM) of band-edge luminescence between 32 nm and 36 nm.

One can observe from the PL emission spectra that the PL output wavelengths corresponding to the emission peaks of CdSe/ZnS core/shell NCs are in the range between 507 nm and 542 nm for different reaction times. The PL emission peaks increase with increasing temperatures.

The first exciton transition energies in UV-Vis optical absorption spectra are known as the core band gaps of both spherical bare CdSe core and CdSe/ZnS core/shell QDs, and they are determined from UV-Vis absorption spectral data shown in Figures 4 and 5 at maximum wavelength according to conventional expression [9].

$$E_g^{nc}(d) = \frac{hc}{\lambda_{max}}, \tag{1}$$

where $E_g^{nc}(d)$ is the core band gap measured at the maximum wavelength λ_{max} at which absorption of nanoparticles is maximum and c and h are, respectively, the speed of light and Planck's constant.

The quantum yield of bare CdSe core and CdSe/ZnS core/shell QDs were calculated by comparing with a standard (Rhodamine-101 in ethanol), with an assumption of its QYs as 95%, and using the data from the fluorescence and absorbance spectra of QDs, estimated using the following expression [10]:

$$\varphi_x = \varphi_s\left(\frac{I_x}{I_s}\right)\left(\frac{A_s}{A_x}\right)\left(\frac{n_x^2}{n_s^2}\right), \tag{2}$$

where I_x (sample) and I_s (standard) are integrated emission peaks, upon 480 nm excitation; A_x (sample) and A_s (standard) are absorption areas at 480 nm; n_x (sample) and n_s (standard) are refractive indices of solvents; and φ_x and φ_s are FL QYs for measured and standard samples. The maximum wavelengths of UV-Vis absorption and PL emission and corresponding Stokes shifts and full width at half maximum (FWHM) for bare CdSe QDs, synthesized from 150°C to 175°C, are given in Table 1 for 5 and 10 minutes of reaction times.

The peak intensity values of UV-Vis absorption and PL emission spectra, Stokes shift, full width at half maximum (FWHM), and quantum yield (QY) of CdSe/ZnS core/shell QDs synthesized at 160°C and 170°C are listed in Table 2 for reaction times between 1 and 20 min., respectively. The fluorescence quantum yield (QY) of CdSe/ZnS core/shell QDs synthesized at 160°C and 170°C increases monotonically from 27% to 45% with reaction time increase and decreases as reaction time is increased further. This result suggests that one can optimize the reaction time to get maximum quantum yield. Furthermore, the FWHM of CdSe/ZnS core/shell QDs synthesized at 170°C (160°C) decreases (increases) as reaction time is increased.

The difference between the first exciton energy of absorption spectra and the PL peak energy in emission spectra at the maximum wavelength is known as the Stokes shift, given as $\Delta E = 2S\hbar\omega_p$, where $\hbar\omega_p$ is the energy of the photon coupled to the electron (25 meV for CdSe), and S is called the Huang-Rhys factor [11], which is the measure of the strength of electron-phonon coupling. Figure 6(a) shows the temperature dependence of the maximum wavelength of absorption and emission spectra and Stokes shift of the bare CdSe core QD as a function of temperature for several reaction times. The maximum wavelength of emission and the absorption spectral data given in Table 2 are used to study the effect of the growth temperature and reaction time on the Stokes shifts in CdSe/ZnS core/shell QD. Figure 6(b) shows the reaction-time dependence of the Stokes shift of CdSe/ZnS core/shell QD synthesized at 160°C and 170°C.

Stokes shift in bare CdSe core NCs is observed to have a parabolic decrease with temperature increase and can be fitted to the following expression:

$$\Delta E(T) = -1.15 \times 10^{-2}T^2 + 4.75T - 436.44, \tag{3}$$

which indicates that increasing temperature decreases the magnitude of the Stokes shift and the corresponding Huang-Rhys factor, due to the increasing effect of the electron-phonon interaction with the temperature increase. Furthermore, the reaction time dependence of the Stokes shift in the spherical CdSe/ZnS core/shell QD synthesized at 160°C and 170°C shown in Figure 6(b) indicates that increasing reaction time has a varying effect on the magnitude of the Stokes shift and the corresponding Huang-Rhys factor.

3.4. Discussion. The conventional two-band effective mass approximation [12] gives a qualitative understanding of the confinement effects on core band gap and diameter of quantum dots. In this model, the solution of the Schrödinger equation for a particle in a spherical box gives the first

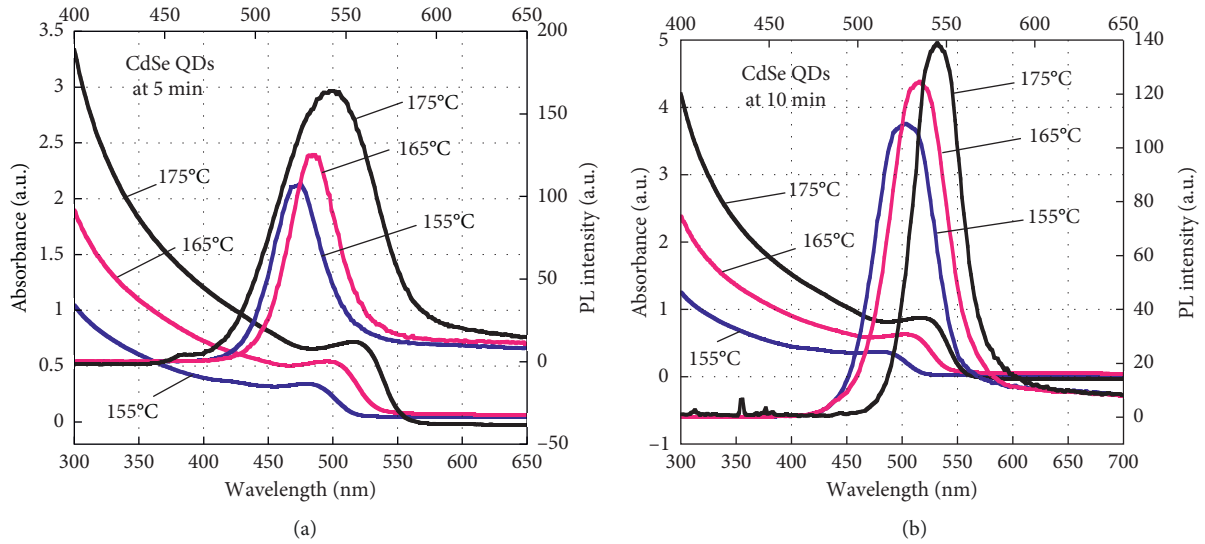

Figure 4: Absorbance and emission spectra of bare CdSe core QDs synthesized at 155°C, 165°C, and 175°C for 5 min (a) and 10 min (b), plotted as a function of photon wavelength.

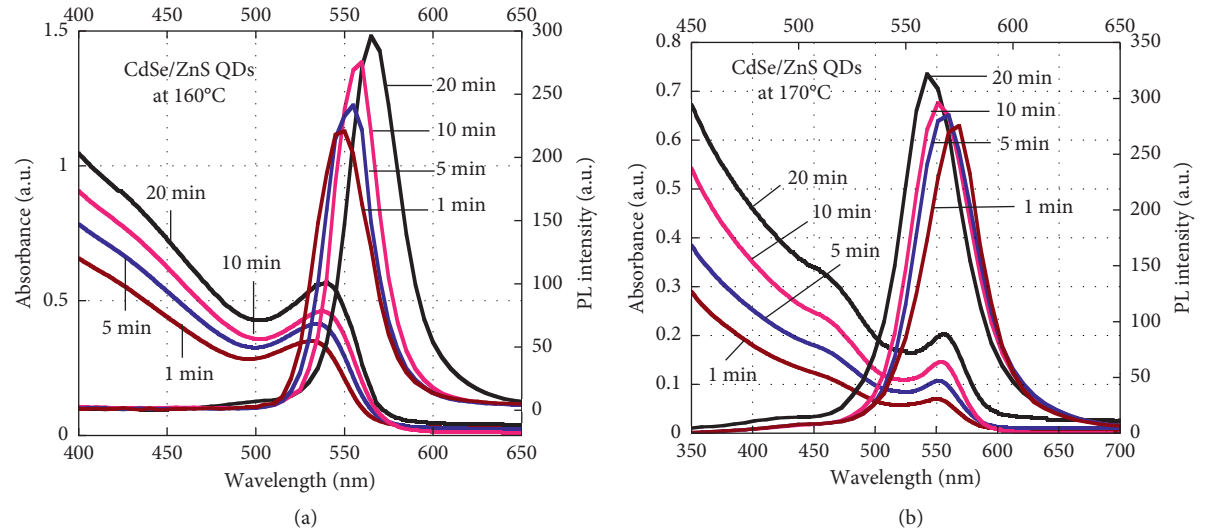

Figure 5: Absorbance and emission spectra of CdSe/ZnS core/shell QDs synthesized at 160°C (a) and 170°C (b) for different reaction times, plotted as a function of photon wavelength.

Table 1: Maximum wavelengths of UV-Vis absorption and PL emission spectra and the corresponding Stokes shift and the full width at half maximum (FWHM) of bare CdSe core QDs at different temperatures for 5 and 10 minutes of reaction times.

Reaction time (min)	Growth temperature (°C)	λ_{max} of absorption spectra (nm)	λ_{max} of emission spectra (nm)	Stokes shift (nm)	FWHM (nm)
5	150	452	521	69	31
	155	476	525	49	33
	160	484	527	43	42
	165	496	532	36	65
	170	508	538	30	43
	175	512	541	29	48
10	150	453	525	72	30
	155	481	527	46	32
	160	488	530	42	33
	165	500	535	35	32
	170	512	542	30	44
	175	516	545	29	62

Table 2: Absorption and emission peak intensities, full width at half maximum (FWHM), and quantum yield (QY) of CdSe/ZnS QDs synthesized at 160°C and 170°C and measured at different reaction times.

Temperature (°C)	Time (min)	Peak absorbance wavelength (nm)	Peak emission wavelength (nm)	Stokes shift (nm)	FWHM (nm)	QY (%)
160	1	532	550	18	32	27
	5	535	553	18	33	41
	10	538	554	16	32	45
	20	539	556	17	36	36
170	1	549	560	11	35	28
	5	552	563	11	34	40
	10	555	565	10	33	44
	20	557	570	13	33	42

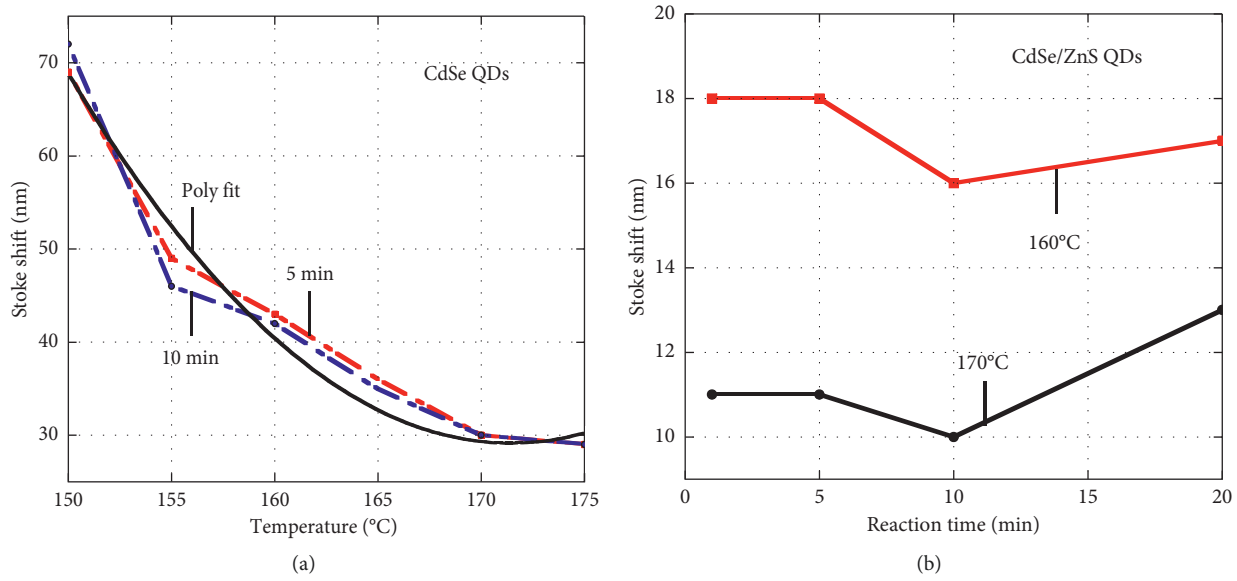

Figure 6: Stokes shift in bare CdSe core QDs (a) as a function of temperature and that in CdSe/ZnS core/shell QDs (b) as a function of reaction time, respectively.

excited state (1s-1s) energy (core band gap) of nanoparticle, given by the following expression:

$$E_g^{nc}(d) = E_g^b + \frac{2\hbar^2\pi^2}{m_{cv}^* d^2} - \frac{3.572e^2}{\varepsilon_\infty d} + \frac{0.124e^4}{\hbar^2 m_{cv}^* \varepsilon_\infty^2}, \quad (4)$$

where E_g^b is the band gap, $m_{cv}^* = m_e^* m_h^*/(m_e^* + m_h^*)$ is the reduced effective mass of the electron-hole pair with effective masses of electrons and holes m_e^* and m_h^*, respectively, and ε_∞ is the optical dielectric constant of CdSe in bulk form. The second and third terms, respectively, represent the confinement energy and the Coulomb interaction energy with a $1/d^2$ and $1/d$ dependence on QD diameter. Finally, the last term is the Rydberg correlation energy, which is negligibly small for when ε_∞ of the semiconductor component is large.

Since spherical core/shell QDs are grown from two semiconductors with different lattice constants and thermal expansion coefficients at temperatures above 300 K, there will be an elastic strain developed across heterointerface. The elastic strain can modify the structural and electronic properties of the core and shell constituents in a way that is not seen in two-dimensional quantum wells and superlattices. In order to understand the strain effects on the structural and electronic properties of bare CdSe core and CdSe/ZnS core/shell QDs, we will use the recent extension of the universal Eshelby's elastic strain model [13] to study the strain effects in nanoscale spherical core/shell heterostructures at any temperature [14–16]. According to this model, one assumes that the core radius is much smaller than that of the shell constituent ($a << b$) of the spherical core/shell heterostructure and writes the interface strain in the core region as [16]

$$\varepsilon_i = \frac{a_i(\varepsilon_i) - a_i}{a_i} = \alpha_i(T)T - \frac{2E_m(1-2\nu_i)[\varepsilon_{im} + (\alpha_i - \alpha_m)T]}{E_i(1+\nu_m) + 2E_m(1-2\nu_i)}, \quad (5)$$

where $\varepsilon_{im} = (a_i - a_m)/a_m$ and $(\alpha_i - \alpha_m)T$ are lattice and thermal mismatches, respectively. Here, a_i and a_m are lattice constants, and α_i and α_m are the linear expansion coefficients of the core and shell at 300 K. E_i (E_m) is Young's modulus and ν_i (ν_m) is Poisson's ratio of the core (shell) semiconductor in bulk form, defined as $E = (C_{11} - C_{12})(C_{11} + 2C_{12})/(C_{11} + C_{12})$ and $\nu = C_{12}/(C_{11} + C_{12})$, where C_{11} and C_{12} are elastic stiffness constants.

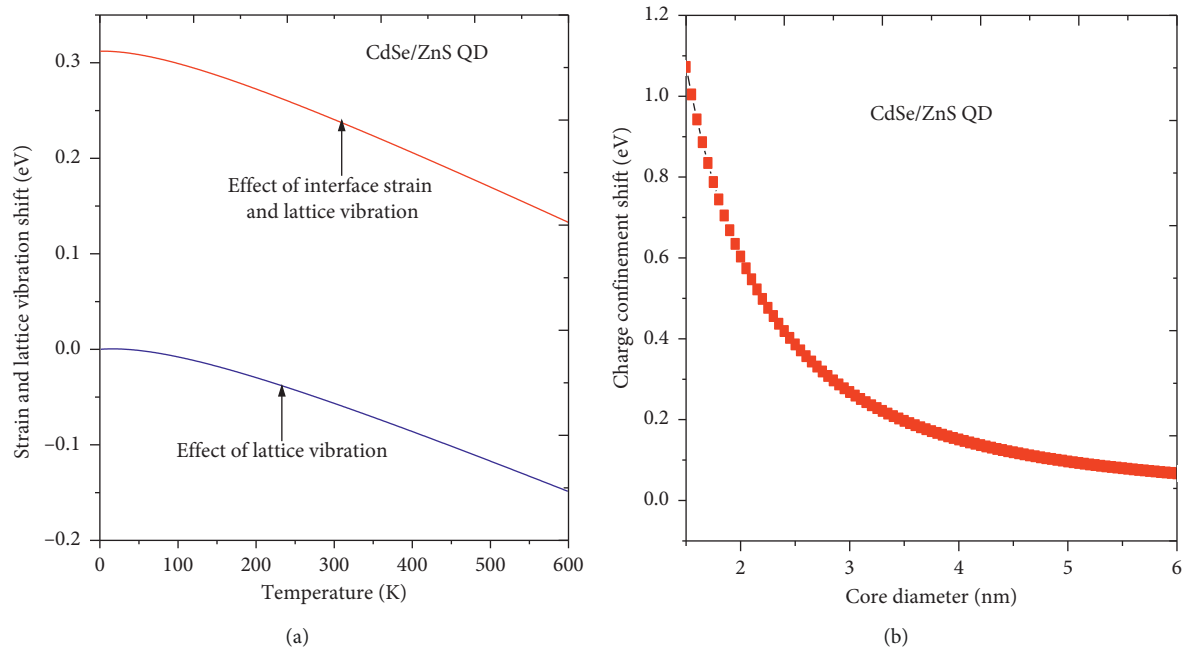

FIGURE 7: Effects of interface strain and electron-phonon interactions (a) and charge confinement effects (b) on band gap decrease of CdSe/ZnS core/shell QDs, respectively.

Using the elastic constants $C_{11} = 10.2$ GPa and 6.67 GPa and $C_{12} = 6.46$ GPa and 4.63 GPa, linear thermal expansion coefficients $\alpha_i = 7.30 \times 10^{-6}\,K^{-1}$, $\alpha_m = 6.9 \times 10^{-6}\,K^{-1}$, and lattice constants $a_i = 0.607$ nm and $a_m = 0.41$ nm for CdSe and ZnS [17], equation (5) gives $\varepsilon_i = -3.70\%$ compressive strain at interface of spherical CdSe/ZnS core/shell QD, which has positive lattice mismatch $\Delta a/a = (a_i - a_m)/a_m = 12.3\%$ at room temperature. Therefore, we can conclude that reliable modelling and precise determination of the magnitude of the strain effects on the electronic structure of nanoscale heterostructures is extremely important for predicting their potential and the simulation of the performance of nanoscale electronic and optical devices. In doing so, one must then modify equation (4) to the following expression in order to take into account the strain effects on the core band gap for a reliable understanding of charge confinement in CdSe/ZnS core/shell QDs [14].

$$E_g^{nc}(\varepsilon_i) = E_g^{bc}(T, \varepsilon_i) + \frac{2\hbar^2\pi^2}{m_{cv}^* d^2} - \frac{3.572e^2}{\varepsilon_\infty d} + \frac{0.124e^4}{\hbar^2 m_{cv}^* \varepsilon_\infty^2}, \quad (6)$$

where $E_g^{bc}(T, \varepsilon_i)$ is the strain-dependent band gap of the core semiconductor in bulk, which is obtained by using a statistical thermodynamic model of semiconductors [18] as

$$E_g^{bc}(T, \varepsilon_i) = E_g^{bc}(0) + \Delta C_{iP}^0 T(1 - \ln T) - \frac{a_{gi}}{B_i}\left(P - \frac{P^2}{2B_i} - \frac{(1 + B_i')}{3B_i^2}P^3\right), \quad (7)$$

where P is the hydrostatic pressure acting on the band structure of the core region, given by

$$P = -3B_i\varepsilon_i(T) = -3B_i\alpha_i(T)\Delta T + 3B_i\frac{2E_m(1 - 2\nu_i)[\varepsilon_{im} + (\alpha_i - \alpha_m)T]}{E_i(1 + \nu_m) + 2E_m(1 - 2\nu_i)}. \quad (8)$$

Logarithmic term $\Delta C_P^0 T(1 - \ln T)$ in equation (7) represents lattice vibration contribution to the band gap change. ΔC_P^0 is the heat capacity of the reaction for formation of the electron-hole pair obtained by fitting the bulk band gap calculated from equation (7) at constant pressure to the measured band gap [18], fitted to

$$E_g^b(T) = E_g^b(0) + \frac{\alpha T^2}{\beta + T}, \quad (9)$$

which is known as Varshni equation [19]. Here $\alpha = 4.09 \times 10^{-4}$ and $\beta = 187$ are constants for bulk CdSe. We can now use equation (7) to get a qualitative understanding of the variation of the core band gap with its diameter at any temperature.

Using the material parameters for CdSe and ZnS bulk semiconductors [17], we calculated the effects of the interface strain, electron-phonon interactions, and charge confinement on the shift in core band gap of bare CdSe core QD and CdSe/ZnS core/shell QD as a function of temperature. Figures 7(a) and 7(b) compare the contribution of the interface strain and electron-phonon interaction (Figure 7(a)) and charge confinement (Figure 7(b)) on band gap decrease in band gaps of CdSe/ZnS core/shell QD. Figure 7(a) indicates that electron-phonon interaction (lattice vibration) contribution to core band gap decrease is always less than zero, and interface strain and lattice vibration tends to decrease core band gap with temperature increase. However, Figure 7(b) indicates that charge

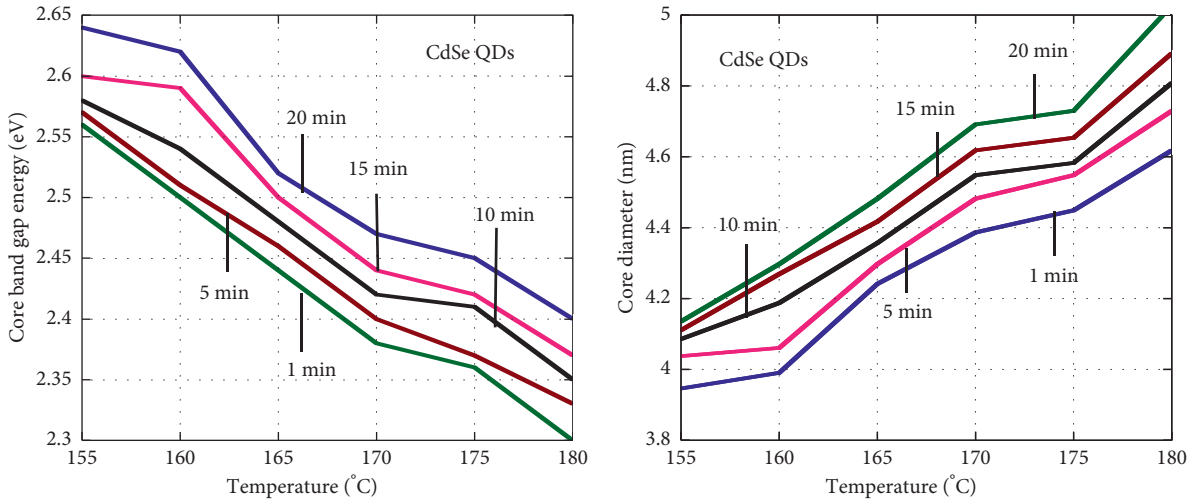

FIGURE 8: Temperature variation of core band gap energy (a) and diameter (b) of bare CdSe core QDs processed at 1, 5, 10, and 20 minutes of reaction times, respectively.

TABLE 3: UV-Vis maximum wavelength and corresponding measured band gap and calculated unstrained and strained core diameter of CdSe/ZnS QDs synthesized at 160°C and 170°C for different reaction times (min).

Temperature (°C)	Time (min)	λ_{max} (nm)	E_g^{nc} (eV)	d (nm)	$d(\varepsilon_i)$ (nm)
160	1	532	2.34	3.89	4.35
	5	535	2.32	3.92	4.39
	10	538	2.31	3.95	4.43
	20	539	2.30	3.96	4.45
170	1	549	2.26	4.02	4.61
	5	552	2.25	4.05	4.66
	10	555	2.23	4.08	4.71
	20	557	2.23	4.11	4.74

confinement has parabolic dependence on the core diameter and becomes nearly flat as the core diameter is increased above 6 nm.

Once first exciton energy (core bad gap) is determined from the UV-Vis absorption data using equation (1), core diameter quantum dot can also be calculated by converting equation (6) to a quadratic equation as d is variable: $Ad^2 + B\,d + C = 0$, where A, B, and C are material parameter-dependent coefficients. The positive root of such quadratic equation will give the diameter of QDs. This will then allow one to calculate the core diameter of the bare core and core shell QDs from the first excited state energy extracted from UV-Vis absorption spectra. Figures 8(a) and 8(b) show the measured core band gaps and calculated diameter of bare CdSe core QDs synthesized at temperatures between 155°C and 180°C and processed at 1, 5, 10, 15, and 20 minutes, respectively.

A polynomial fit to the core band gap of bare CdSe QDs, processed at 5 min, suggests a parabolic temperature of the core band gap given as

$$E_g^{nc}(T) = aT^2 + bT + c, \tag{10}$$

where a, b and, c are coefficients, which can be strain- and temperature-dependent. The parabolic fit in Figure 8(a) yields $a = 4.43 \times 10^{-4}\,K^{-2}$, $b = -0.16\,K^{-1}$, and $c = 16.26$ for 10 minutes of reaction time. The parabolic decrease of the core band gap of bare CdSe QDs with temperature increase shown in Figures 8(a) and 8(b) is consistent with the fact that the band gap of most of the group IV elemental and groups III–V and II–VI compound semiconductors tends to decrease with increasing temperature, due to electron-phonon interaction and free expansion of the lattice constant with increasing temperature. Similar polynomial fit to the core diameter of CdSe QD is given by

$$d^{nc}(T) = a^*T^2 + b^*T + c^*, \tag{11}$$

where a^*, b^*, and c^*, d, e, and, f are coefficients, which can be temperature dependent. $a^* = -5.04 \times 10^{-4}/K^2$, $b^* = 0.18/K$, and $c^* = -12.96$ for 10 minutes of reaction time. Since there is only free thermal expansion of lattice constant in bare core QDs, shift in their band gap and diameter is mainly due to electron-phonon interaction with temperature increase.

Since the lattice constant and thermal expansion coefficient of the CdSe core are greater than those of the ZnS shell of CdSe/ZnS core/shell QDs, the CdSe core region will be under compressive strain, resulting in an increase (decrease) in its band gap energy (diameter) as temperature is increased. Table 3 gives list of the UV-Vis maximum wavelength of absorption coefficient and corresponding first excited state energies (core band gaps) of CdSe/ZnS QDs core/shell QDS synthesized at 160°C and 170°C and processed for 1, 5, 10, and 20 minutes, respectively.

Using the results given in Table 3, the unstrained and strained values of core diameters are compared in Figure 9 as a function of the core band gap of CdSe/ZnS core/shell QDs synthesized at 160°C and 170°C for

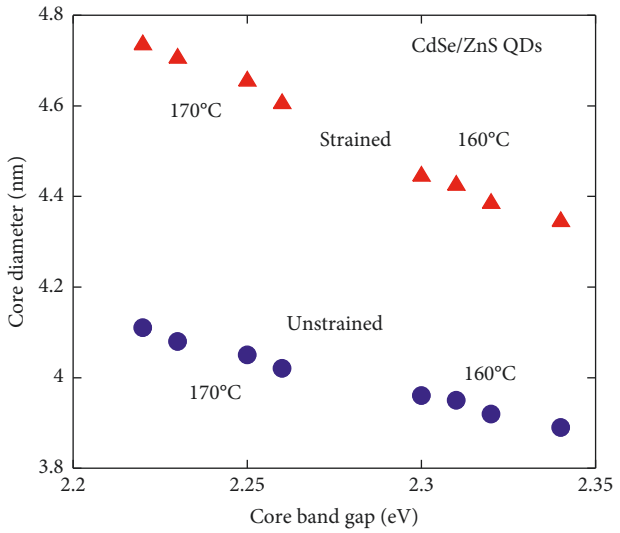

Figure 9: Core diameter of CdSe/ZnS core/shell QDs plotted and as a function of core band gap with and without strain at 160°C and 170°C, respectively.

various reaction times, respectively. Calculated unstrained and strained diameters show a parabolic decrease (increase) as core band gap increase (decreases) at both temperatures.

The strained core diameters are in excellent agreement with HRTEM results, which indicates that the bare CdSe core and core/shell CdSe/ZnS QDs synthesized at 160°C and 170°C for 20 minutes of reaction time have average particle sizes about 3.50 nm and 4.84 nm, respectively.

4. Conclusion

We presented the results of a comprehensive study of elastic strain effects on the core band gap and diameter of spherical bare CdSe core and CdSe/ZnS heterostructure core/shell quantum dots that are synthesized by a colloidal technique at various temperatures. The XRD analysis suggests that the synthesized CdSe core and CdSe/ZnS core/shell QDs have a zinc-blende crystal structure. HRTEM measurements indicate that the bare CdSe core and CdSe/ZnS core/shell QDs have average particle sizes about 3.50 nm and 4.84 nm, respectively. UV-Vis absorption spectra measurements show that the increase of growth temperature leads to a decrease (increase) in the band gap (diameter) of CdSe/ZnS core/shell QDs. Furthermore, we also show that the effect of elastic strain to the band gap change is greater than that of lattice vibration in CdSe/ZnS core/shell QDs at any temperature. The compressive strain causes an increase (decrease) in the core band gap (diameter) of spherical CdSe/ZnS core/shell QDs. Elastic strain–modified effective mass approximation predicts that there is a parabolic decrease (increase) in the core band gap (diameter) of CdSe/ZnS core/shell QDs with temperature. The calculated core diameter of bare CdSe core and CdSe/ZnS core/shell QDs are in excellent agreement with HRTEM measurements.

Data Availability

The data used to support the findings of this study are included within the article.

Conflicts of Interest

The authors declare that they have no conflicts of interest.

Acknowledgments

The authors greatly acknowledge the financial support by the Research Foundation of İstanbul Technical University (İTÜ BAP Project No: 34537). Preliminary part of this work was presented at the Turkish Physical Society 33rd International Physics Congress (TPS-33): AIP Conference Proceedings 1935, 050004 (2018).

References

[1] H. Ünlü, N. J. M. Horing, and J. Dabrowski, *Low Dimensional and Nanostructured Materials and Devices*, Springer, Berlin, Germany, 2015.

[2] H. Zhu, A. Prakash, D. Benoit, C. Jones, and V. Colvin, "Low temperature synthesis of ZnS and CdZnS shells on CdSe quantum dots," *Nanotechnology*, vol. 21, no. 25, Article ID 255604, 2010.

[3] A. Nadarajah, T. Smith, and R. Könenkamp, "Improved performance of nanowire-quantum-dot-polymer solar cells by chemical treatment of the quantum dot with ligand and solvent materials," *Nanotechnology*, vol. 23, no. 48, p. 485403, 2012.

[4] C.-Y. Huang, Y.-K. Su, T.-C. Wen, T.-F. Guo, and M.-L. Tu, "Single-layered hybrid DBPPV-CdSe-ZnS quantum-dot light-emitting diodes," *IEEE Photonics Technology Letters*, vol. 20, no. 4, pp. 282–284, 2008.

[5] L. Deng, L. Han, Y. Xi, X. Li, and W. P. Huang, "Design optimization for high-performance self-assembled quantum dot lasers with fabry–perot cavity," *IEEE Photonics Journal*, vol. 4, no. 5, pp. 1600–1609, 2012.

[6] W. Luan, H. Yang, N. Fan, and S.-T. Tu, "Synthesis of efficiently green luminescent CdSe/ZnS nanocrystals via microfluidic reaction," *Nanoscale Research Letters*, vol. 3, no. 4, pp. 134–139, 2008.

[7] R. He and H. Gu, "Synthesis and characterization of mondispersed CdSe nanocrystals at lower temperature," *Colloids and Surfaces A: Physicochemical and Engineering Aspects*, vol. 272, no. 1-2, pp. 111–116, 2006.

[8] C.-Q. Zhu, P. Wang, X. Wang, and Y. Li, "Facile phosphine-free synthesis of CdSe/ZnS core/shell nanocrystals without precursor injection," *Nanoscale Research Letters*, vol. 3, no. 6, pp. 213–220, 2008.

[9] S. Suresh, "Studies on the dielectric properties of CdS nanoparticles," *Applied Nanoscience*, vol. 4, no. 3, pp. 325–329, 2013.

[10] M. Grabolle, M. Spieles, V. Lesnyak, N. Gaponik, A. Eychmüller, and U. Resch-Genger, "Determination of the fluorescence quantum yield of quantum dots: suitable procedures and achievable uncertainties," *Analytical Chemistry*, vol. 81, no. 15, pp. 6285–6294, 2009.

[11] A. Joshi, K. Y. Narsingi, M. O. Manasreh, E. A. Davis, and B. D. Weaver, "Temperature dependence of the band gap of colloidal core/shell nanocrystals embedded into an ultraviolet

curable resin," *Appl. Phys. Lett.*vol. 89, no. 13, Article ID 131907, 2006.

[12] L. E. Brus, "Electron-electron and electron-hole interactions in small semiconductor crystallites: the size dependence of the lowest excited electronic state," *The Journal of Chemical Physics*, vol. 80, no. 9, pp. 4403–4409, 1984.

[13] J. Eshelby, "The determination of the elastic field of an ellipsoidal inclusion, and related problems," *Proceedings of the Royal Society of London. Series A. Mathematical and Physical Sciences*, vol. 241, no. 1226, pp. 376–396, 1957.

[14] H. Ünlü, "Modelling of CdSe/CdZnS and ZnSe/CdZnS binary/ternary heterostructure core/shell quantum dots," *AIP Conference Proceedings*, , vol. 1935, Article ID 050003, 2018.

[15] M. R. Karim and H. Ünlü, "Temperature and strain effects on core bandgap and diameter of bare CdSe core and CdSe/ZnS heterostructure core/shell quantum dots," *AIP Conference Proceedings*, , vol. 1935, Article ID 050004, 2018.

[16] H. Ünlü, "A thermoelastic model for strain effects on bandgaps and band offsets in heterostructurecore/shell quantum dots," *The European Physical Journal Applied Physics*, vol. 86, no. 3, Article ID 30401, 2019.

[17] O. Madelung, Ed., *Numerical Data and Functional Relationships in Science and Technology, Part d of Vol. 17, (1984)*, Springer, Berlin, Germany.

[18] H. Ünlü, "A thermodynamic model for determining pressure and temperature effects on the bandgap energies and other properties of some semiconductors," *Solid-State Electronics*, vol. 35, no. 9, pp. 1343–1352, 1992.

[19] Y. P. Varshni, "Temperature dependence of the energy gap in semiconductors," *Physica*, vol. 34, no. 1, pp. 149–154, 1967.